

This item was submitted to Loughborough's Institutional Repository (<https://dspace.lboro.ac.uk/>) by the author and is made available under the following Creative Commons Licence conditions.



CC creative commons
COMMONS DEED

Attribution-NonCommercial-NoDerivs 2.5

You are free:

- to copy, distribute, display, and perform the work

Under the following conditions:

BY: **Attribution.** You must attribute the work in the manner specified by the author or licensor.

Noncommercial. You may not use this work for commercial purposes.

No Derivative Works. You may not alter, transform, or build upon this work.

- For any reuse or distribution, you must make clear to others the license terms of this work.
- Any of these conditions can be waived if you get permission from the copyright holder.

Your fair use and other rights are in no way affected by the above.

This is a human-readable summary of the [Legal Code \(the full license\)](#).

[Disclaimer](#) 

For the full text of this licence, please go to:
<http://creativecommons.org/licenses/by-nc-nd/2.5/>

Model of the evolution of acoustic emission as the randomization of transient processes in coupled nonlinear oscillators

V. V. Krylov, P. S. Landa, and V. A. Robsman

M. V. Lomonosov State University, Moscow

(Submitted May 5, 1992)

Akust. Zh. 39, 108-122 (January-February 1993)

The behavior of a crack as a resonator radiating acoustic emission (AE) pulses at instants of sudden growth is investigated theoretically and experimentally. This resonance behavior of a growing crack is determined to a large extent by surface waves propagating along its edges. The crack can therefore be regarded as an acoustic resonator excited at the instant of growth of its tip. Transformations in the form of high-frequency harmonic and combination-frequency subharmonic generation are observed in the spectra of the AE signals. The final stage in the evolution of AE is characterized by the transition to a wideband noise spectrum. These facts lead to the hypothesis that bifurcations analogous to those encountered in the onset of dynamic chaos take place in the AE process. This hypothesis forms the basis of a mathematical model of the AE process as a system of coupled nonlinear oscillators, each corresponding to an individual crack. The initial displacement in one of the interacting cracks is adopted as the bifurcation parameter. Spectra calculated by computer simulation exhibit qualitative agreement with the evolution of the spectra obtained in the processing of data from physical experiments.

Irreversible fracture processes in materials are known to be accompanied by a characteristic pulsed acoustic radiation, or acoustic emission (AE). The sources of the AE signals are the growing cracks themselves.

A numerical solution of the problem of the dynamics and radiation from a finite crack subjected to tensile stresses shows¹ that the instantaneous application of a load to the edge of a crack causes it to open up and move by an oscillating route to the next static position. This suggests that the response of the crack to an applied force is a resonance phenomenon. The same conclusion can be drawn on the basis of an analysis of the numerical solution of the problem of the dynamics of the edges of a crack subjected to a harmonic exciting force²; according to the analysis, the frequency ω_0 of maximum response depends only on the dimensions of the formative crack and on the elastic properties of the medium. For example, if the Poisson ratio is $\nu = 0.25$, we find that $\omega_0 \approx C_l/2l$, where C_l is the longitudinal wave velocity, and $2l$ is the length of the crack. Unfortunately, definite conclusions as to the nature of the resonances cannot be made on the basis of these numerical calculations. However, it is readily verified that the resonance behavior of the crack is determined to a large extent by Rayleigh surface waves propagating along its edges.

We consider a two-dimensional crack of length $2l$, which is situated in a medium subjected to uniform tensile stresses $\sigma(t)$.

According to Ref. 3, the spectrum of normal displacements generated by the expanding crack can be described by means of the integral representation

$$U_z(x, z, \omega) = \int_{-\infty}^{\infty} \sigma_{zz}(\xi, \omega) G_{zz}^0(z, x - \xi, \omega) d\xi, \quad (1)$$

where $U_z(x, z, \omega)$ is the z -component of the displacement spectrum in the body, $\sigma_{zz}(x, \omega)$ is the spectrum of normal elastic stresses acting in the plane $z = 0$ drawn through the crack, and $G_{zz}^0(z, x - \xi, \omega)$ is the corresponding component of the dynamic Green's tensor for free-surface boundary conditions. According to Eq. (1), it is necessary to know the stress σ_{zz} in the entire plane $z = 0$ in order to determine the dis-

placements of the edges of the crack, i.e., the values of $U_z^0 = U_z(z = 0)$ at $|x| < l$. However, because of the mixed boundary conditions in the plane of the crack, σ_{zz} is known only at $|x| < l$, where it is required to set $\sigma_{zz}(\omega) = -\sigma(\omega)$ [$\sigma(\omega)$ is the temporal spectrum of the tensile stresses]. The values of σ_{zz} at $|x| \geq l$ can be determined by means of an integral equation, which is readily obtained from Eq. (1) through one of the boundary conditions in the plane $z = 0$, specifically the condition that the normal displacements U_z^0 are equal to zero for $|x| \geq l$. With this in mind, we can write the required integral equation in the form

$$\int_{-l}^l \sigma(\omega) G_{zz}^0(x - \xi, \omega) d\xi = \int_{-\infty}^{-l} \sigma_{zz}^*(\xi, \omega) G_{zz}^0(x - \xi, \omega) d\xi + \int_l^{\infty} \sigma_{zz}^*(\xi, \omega) G_{zz}^0(x - \xi, \omega) d\xi, \quad (2)$$

where σ_{zz}^* denotes the unknown values of the stresses σ_{zz} at $|x| \geq l$, and $\sigma(\omega) = (1/2\pi) \int_{-\infty}^{\infty} \sigma(t) \exp(i\omega t) dt$ is the spectrum

of tensile stresses. Equation (2) has the physical significance that the tensile stresses $\sigma(\omega)$ acting in the region $|x| \geq l$ create a field of sources σ_{zz}^* , which generates in this region a displacement field opposite to the field generated directly by the forces $\sigma(\omega)$ localized in the zone $|x| < l$. Taking the symmetry of the problem into account: $\sigma_{zz}^*(-\xi) = \sigma_{zz}^*(\xi)$, we can rewrite Eq. (2) in the form

$$\int_l^{\infty} \sigma_{zz}^*(\xi, \omega) K(x, \xi, \omega) d\xi = \Phi(x, \omega), \quad (3)$$

where the kernel is given by the expression

$$K(x, \xi, \omega) = G_{zz}^0(x - \xi, \omega) + G_{zz}^0(x + \xi, \omega),$$

and

$$\Phi(x, \omega) = \sigma(\omega) \int_{-l}^l G_{zz}^0(x - \xi, \omega) d\xi.$$

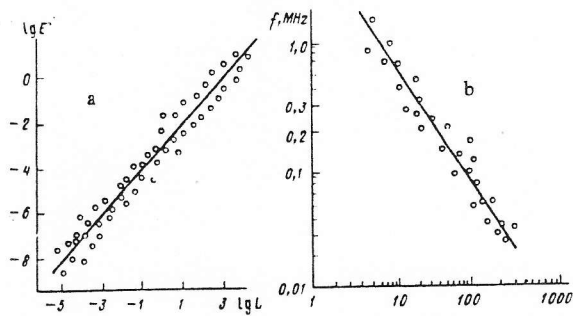


FIG. 1. Empirical graphs of parameters of AE signals vs the length L of formative cracks. a) AE signal energy E ; b) dominant frequency f in the AE signal spectra.

We note that Eq. (3) is exact and represents a Fredholm integral equation of the first kind. The component of the Green's tensor G_{zz}^0 used in Eq. (3) has the form

$$G_{zz}^0(x - \xi, z = 0) = (1/2\pi) \int_{-\infty}^{\infty} (V_1 M e^{-v_1 z} + ik N l^{-v_1 z}) e^{ik(x-\xi)} dk, \quad (4)$$

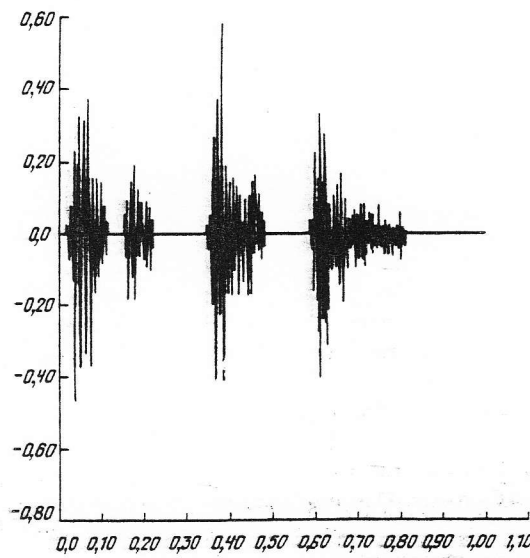


FIG. 2. Solitary AE pulses recorded at instants of discrete crack growth.

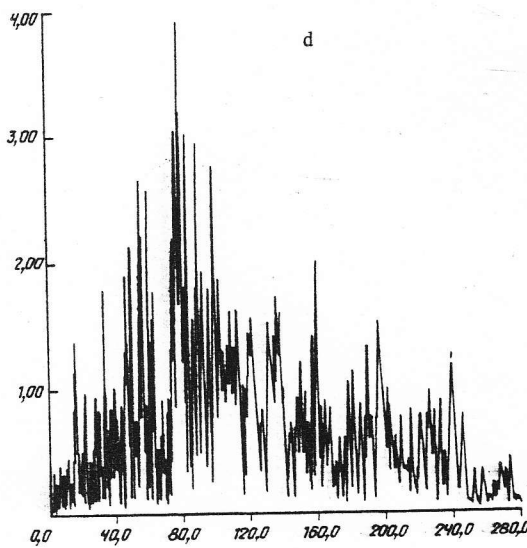
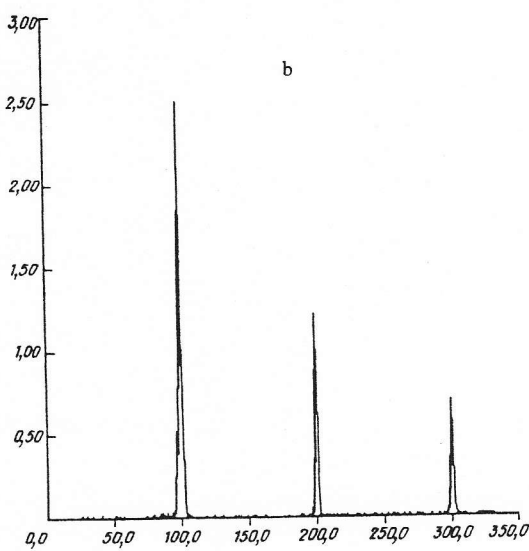
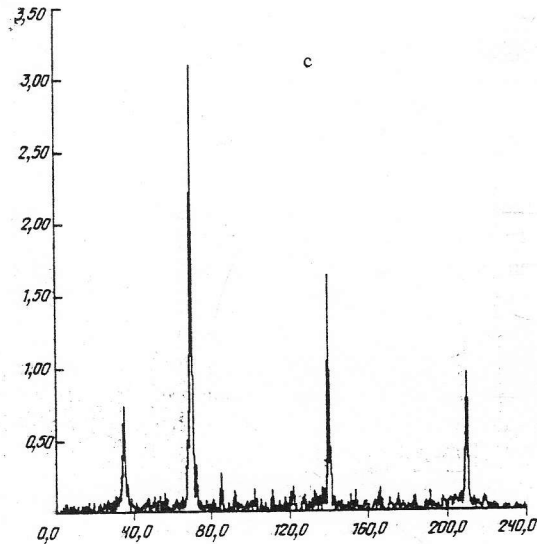
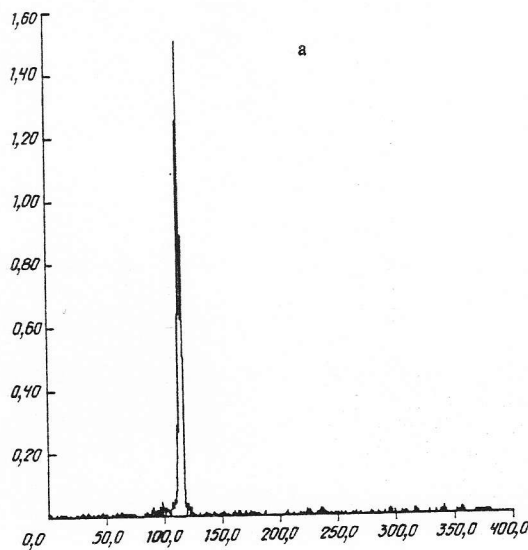


FIG. 3. Nonlinear spectral variations during the evolution of acoustic emission with the formation of an even subharmonic (from a physical experiment on the fracture of a composite material). a) Narrowband AE signal spectrum; b) AE signal spectrum with high-frequency harmonic components; c) AE signal spectrum with an even subharmonic; d) continuous wideband AE signal spectrum.

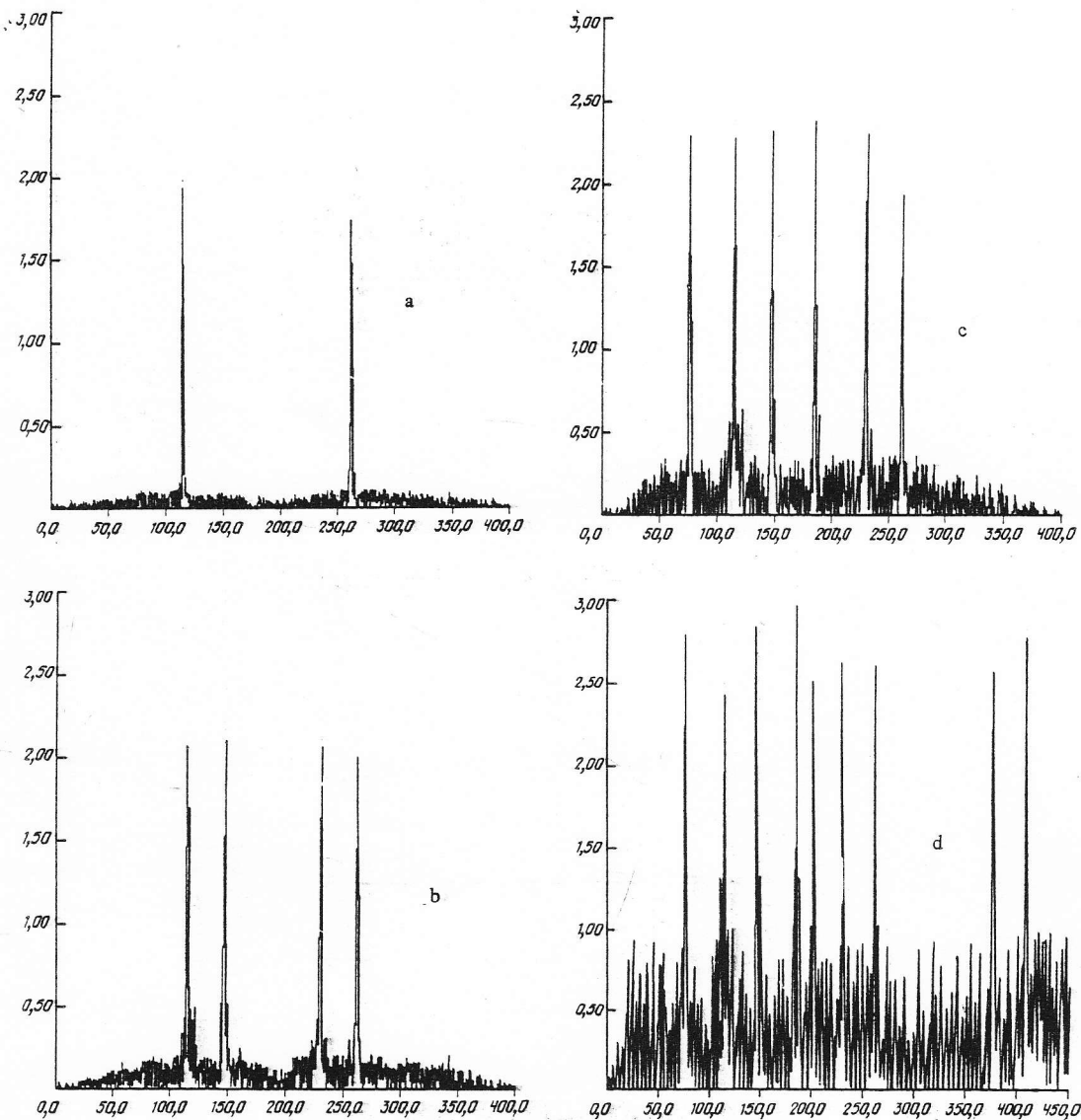


FIG. 4. Nonlinear spectral variations during the evolution of acoustic emission with the formation of an even subharmonic (from a physical experiment on the fracture of reinforced concrete). a) $f = 115$ kHz, 262 kHz; b) 115, 262, 147, 230; c) 115, 262, 147, 230, 77, 185; d) 115, 262, 147, 230, 77, 185, 377, 202, 409 kHz.

where $M = -(2k^2 - k_t^2)/\mu F(k)$, $N = 2ikV_l/\mu F(k)$, $V_{l,t} = (k^2 - k_{l,t}^2)^{1/2}$, k_l and k_t are the longitudinal and transverse wave numbers, $F(k) = (2k^2 - k_t^2)^2 - 4k^2V_lV_t$ is the so-called Rayleigh determinant, and μ is the shear modulus. The direct substitution of the Green's function (4) in Eq. (3) excludes its analytical solution for all practical purposes, because the integral in Eq. (4) can be evaluated analytically only in the far field. The corresponding asymptotic expansion of the Green's function has the form

$$G_{zz}^0(x - \xi) = A \exp(ik_R |x - \xi|) + B |(k_l |x - \xi|)^{-3/2} C \exp(ik_l |x - \xi|) + (k_t |x - \xi|)^{-3/2} D \exp(ik_t |x - \xi|) + \dots \quad (5)$$

where A , B , C , and D are constants, which depend on the Poisson ratio of the medium, and k_R is the Rayleigh wave number, which is the real root of the equation $F(k) = 0$. The first term in Eq. (5) represents a Rayleigh surface wave, and the second and third terms represent rapidly decaying longitudinal and transverse bulk waves propagating along the surface $z = 0$.

Since we are interested primarily in resonance phenomena, which we shall consider to be associated with Rayleigh waves propagating along the edges of a crack, it is natural to keep only the Rayleigh branch [the first term of the expansion (5)] in the Green's function G_{zz}^0 ; this makes sense for any $|x - \xi|$, despite the asymptotic character of Eq. (5). In other words, we represent the Green's function by the approximate expression

$$G_{zz}^0(x - \xi) = A \exp(ik_R |x - \xi|). \quad (6)$$

We see at once that the coefficient A enters into both sides of the integral equation (3) as a factor. We therefore drop it in the solution. The substitution of Eq. (6) in Eq. (3) reduces the latter to the form

$$\int_l^\infty \sigma_{zz}^*(\xi, \omega) [\exp(ik_R |x - \xi|) + \exp(ik_R (x + \xi))] d\xi = [2\sigma(\omega)/k_R] \sin k_R l \cdot \exp(ik_R x), \quad x > l. \quad (7)$$

It is interesting that the simplified equation (7) is solved

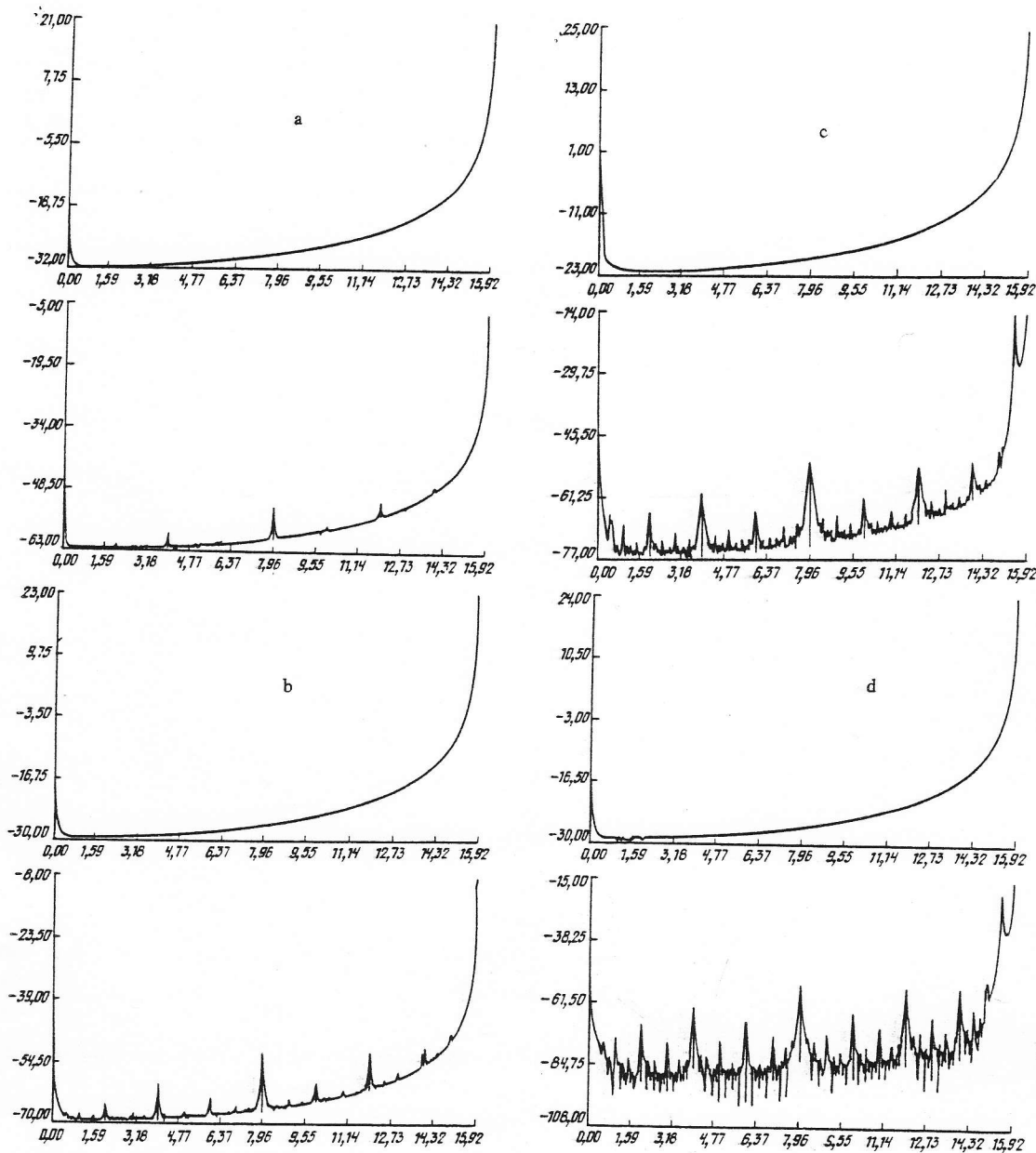


FIG. 5. Results of the numerical simulation of two coupled nonlinear oscillators ($a_1 = a_2 = 0.5$, $b = 10$) for various values of the bifurcation parameter x . a) $x = 0.1$; b) $x = 0.14$; c) $x = 0.21$; d) $d = 0.24$.

exactly. Let us assume, in fact, that the solution σ_{zz}^* has the form⁴

$$\sigma_{zz}^*(x, \omega) = f(\omega) \delta(x - l), \quad (8)$$

where $f(\omega)$ is a function yet to be determined and $\delta(x - l)$ is the Dirac delta function, and let us substitute Eq. (8) in (7). It is readily verified by appropriate transformations that Eq. (7) is satisfied if

$$f(\omega) = (2\sigma(\omega)/k_R) \operatorname{tg}(k_R l).$$

Consequently, the total distribution of the unknown stresses beyond the limits of the crack (at $|x| > l$) is

$$\sigma_{zz}^*(x, \omega) = (2\sigma(\omega)/k_R) \operatorname{tg}(k_R l) [\delta(x - l) + \delta(x + l)]. \quad (9)$$

The quantities of interest, i.e., the normal displacements of the edges of the crack, are readily calculated by means of Eq. (9) and the integral representation (1), in which we need to set $z = 0$. Making use of the fact that $\sigma_{zz}(\omega) = -\sigma(\omega)$ at $|x| < l$ and going through simple but rather cumbersome transformations, we obtain

$$U_z^0(x, \omega) = \frac{2iA(\omega)}{k_R} \left(1 - \frac{\cos k_R x}{\cos k_R l}\right), \quad |x| < l. \quad (10)$$

We recall that $U_z^0(x, \omega) = 0$ at $|x| \geq l$ as a result of the boundary conditions, which follow from the symmetry of the problem about $z = 0$.

It is readily perceived that the amplitude $U_z^0(x, \omega)$ in Eq. (10) becomes infinite for $k_R l = \pi/2 + \pi n$, $n = 0, 1, 2, \dots$, or for $(\lambda_R/2)(2n + 1) = 2l$, indicating the onset of resonance.

The existence of only odd resonances in this case is a consequence of the symmetry of the problem. Thus, within the very crude approximation used here, a crack of length $2l$ is a resonator something like a two-mirror Fabry—Perot interferometer with resonance frequencies $\omega_n = \pi C_R/2l - (2n + 1)$, where $C_R = \omega/k_R$ is the Rayleigh wave phase velocity. The reflection coefficient R for two surface waves propagating along the edges (we call this wave pair a symmetric Rayleigh mode for brevity) from the tip of the crack is equal to -1 in the given approximation. In accordance with the well-known resonance condition for a two-mirror resonator:

$$\frac{\omega}{C_R} 2l + \tilde{\Psi} = \pi n, \quad (11)$$

where $\tilde{\Psi}$ is the phase shift of the symmetric Rayleigh mode in reflection, and n is an integer, we at once deduce the above relation $\omega_n = (\pi C_R/2l)(2n + 1)$. The fact that the displacement amplitudes U_z^0 become infinite at resonance is evidence of the crudeness of the approximate model used here, in which damped bulk acoustic waves and their associated losses, i.e., losses in acoustic radiation from the oscillating crack or in acoustic emission *per se*, are completely ignored (formally, this assumption is a consequence of the relation $|R| = 1$).⁵

The inverse Fourier transformation of Eq. (10) is needed in order to obtain a time-dependent solution $U_z^0(x, t)$. We calculate $U_z^0(x, t)$ for the important special case of an instantaneously applied load $\sigma(t) = \sigma_0 h(t)$, which simulates instantaneous crack formation [here $h(t)$ is the Heaviside unit step function]. We now have $\sigma(\omega) = i\sigma_0/2\pi\omega$, and the expression for $U_z^0(x, t)$ has the form

$$U_z^0(x, t) = -\frac{\sigma_0 A C_R}{\pi} \int_{-\infty}^{\infty} \frac{1}{\omega^2} \left[1 - \frac{\cos(\omega x/C_R)}{\cos(\omega l/C_R)} \right] e^{-i\omega t} d\omega. \quad (12)$$

Using the well-known representation⁶

$$\frac{1}{\cos \beta \omega} = \sum_{j=-1}^{\infty} \frac{(-1)^j}{\beta \omega - (2j-1)\pi/2},$$

we calculate the integral (12) by the method of residues. As a result of this operation and several simple transformations, we find that at $t \geq 0$

$$U_z^0(x, t) = \frac{8\sigma_0 A \pi C_R}{l} \sum_{j=1}^{\infty} \frac{(-1)^{j+1} \cos[(2j-1)(\pi x/2l)]}{[(2j-1)(\pi C_R/2l)]^2} \sin[(2j-1) \frac{\pi C_R}{2l} t]. \quad (13)$$

It follows from Eq. (13) that the displacements of the edges of the crack represent the superposition of undamped modes with resonance frequencies $\omega_j = \pi C_R/2l(2j - 1)$, $j = 1, 2, \dots$, in the given approximation, i.e., without radiation losses. We see at once that the amplitudes of the corresponding normal modes (harmonics) are proportional to $1/\omega_j^2$ for an external excitation in the form of a step function. We shall therefore include the mode at the fundamental resonance $\omega_0 = \pi C_R/2l$ in the ensuing discussion. This value of the fundamental frequency ω_0 is approximately 1.5 times the values calculated numerically.² The difference is attributable to the fact that radiation of bulk waves by the crack is not taken into account. Another consequence of this omission, as already mentioned, is the excursion of the amplitude to infinity [or, related to this, the infinite Q

of the crack as a resonator and the fact that the oscillations are damped in Eq. (13)]. Moreover, the given model does not describe the monotonic opening of the crack to its static position.

We note that the omission of the complete Green's function from Eq. (3) and the subsequent numerical solution of this equation on a computer⁴ yield results consistent with numerical calculations^{1,2} by other methods.

It follows from Eq. (13) that the fundamental frequency of the excited waves becomes lower, and their energy increases as the crack grows; this relationship has been confirmed by appropriate experiments (Fig. 1).

Consequently, the crack can in fact be regarded as a certain acoustic resonator driven at the instant when the tip of the crack grows larger. Indeed, physical experiments show that the AE signals are in the form of isolated trains of damped oscillations, whose occurrence correlates with discrete times of crack growth (Fig. 2). The evolution of the AE signal spectra with increasing load has the following characteristics.

When microdefects originate in the material in the initial stage of loading, the AE signal spectrum represents a narrow line, whose maximum occurs at relatively high ultrasonic frequencies (Fig. 3a). As the defects enter subsequent stages of growth and interact, transformations are observed in the AE spectra in that the maximum shifts into a lower frequency range. This process is accompanied by the onset of high-frequency harmonic components in the spectrum (Fig. 3b).

With a further increase in the external load, an even subharmonic component is formed in the AE signal spectra (Fig. 3c), and in the final stage of active fracture the spectrum becomes continuous and wideband (Fig. 3d). The stage involving the formation of a wideband noise spectrum is preceded by the onset of multiple-frequency even harmonics in some cases and by the onset of combination frequencies in other cases (Fig. 4).

These facts lead to the assumption that the evolution of AE is accompanied by bifurcations analogous to those encountered in the inception of dynamic chaos. This hypothesis provides the foundation of a mathematical model of AE in the form of a system of coupled nonlinear oscillators, each corresponding to an individual crack.

The initial displacement in one of the interacting oscillators can be adopted as the bifurcation parameter. Stepped increments of the bifurcation parameter simulate the growth of one of the interacting cracks.

The coupling of the oscillators simulates the coupling of the cracks through radiation. The oscillators are made quadratically nonlinear by virtue of the fact that the elasticity of a crack in tension is substantially smaller than in compression.

To avoid further complications of the model, we consider two oscillators, assuming that their coupling and the damping forces are linear and that the coupling and damping coefficients and the eigenfrequencies of the oscillators are constants.

The equations of this model can be written in the form

$$\begin{aligned} \ddot{x} + 2h_1 \dot{x} + \omega_1^2(x + a_1 x^2) + by &= 0, \\ \ddot{y} + 2h_2 \dot{y} + \omega_2^2(y + a_2 y^2) + bx &= 0. \end{aligned} \quad (14)$$

We choose the initial displacement of the first oscillator as the bifurcation parameter. We track its influence on the structural transformation of the dynamic regime of nonlinear oscillations on the basis of the corresponding spectral variations.

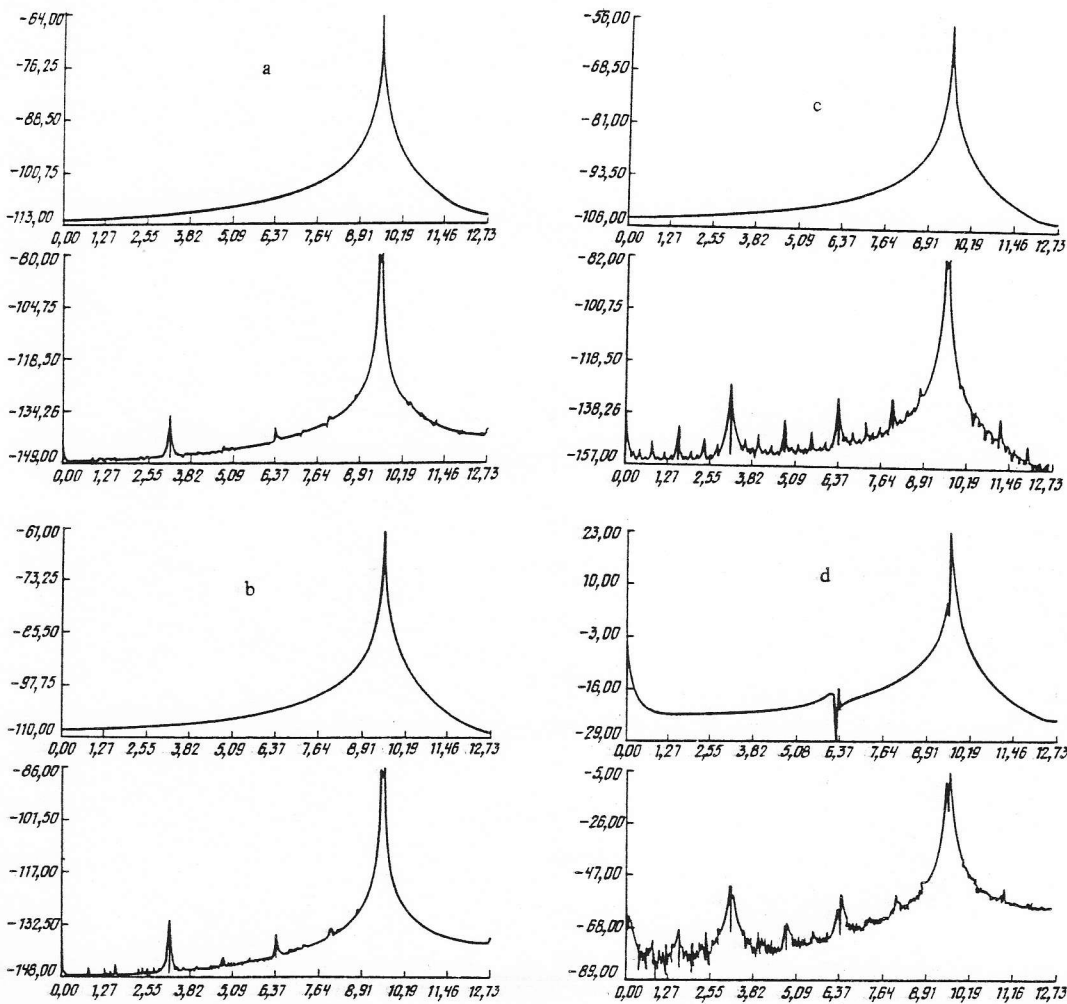


FIG. 6. Results of the numerical simulation of two coupled nonlinear oscillators ($a_1 = a_2 = 0.5$, $b = 0.5$) for various values of the bifurcation parameter x . a) $x = 0.03$; b) $x = 0.05$; c) $x = 0.08$; d) $d = 0.11$.

This approach enables us to explain certain transformations previously observed in AE signal spectra in physical experiments.

A numerical simulation of the system (14) has shown that when the initial displacement of the first oscillator is increased, and provided that the coupling coefficient b is sufficiently large ($b > b_{cr} \approx 1$), the spectrum of the second oscillator acquires the second subharmonic, whereas the spectrum of the first oscillator changes very little (Fig. 5a).

A further increase in the initial displacement of the first oscillator is accompanied by an increase in the number of even subharmonics of the second oscillator. The spectrum of the first oscillator still does not contain any subharmonics (Figs. 5b and 5c).

When the control parameter exceeds a certain critical value, the spectrum of the second oscillator becomes continuous (Fig. 5d). The spectrum of the first oscillators still does not exhibit any visible changes.

It is evident from Fig. 5 that the transition to a continuous spectrum in the second oscillator is analogous to the transition to chaos as a consequence of a series of period-doubling bifurcations. In our case, however, these bifurcations are instigated by a transient rather than a periodic process, where the number of bifurcations appears to be finite. A numerical experiment

has disclosed that the number of such bifurcations increases as the damping of each oscillator decreases. The calculated values of the bifurcation parameter have been used to calculate constants analogous to the Feigenbaum constant. They are found to depend on the damping coefficient $h = h_1 = h_2$:

Damping coefficient	Number of bifurcations	Convergence constant
h	n	δ
0.3	4	2.375
0.03	4	4.611
0.003	5	9.179
0.0003	6	11.237

The spectra obtained for the second oscillator agree qualitatively with the AE signal spectra in Fig. 3.

The transition to chaos proceeds differently if the coupling coefficient b is smaller than b_{cr} . As the initial displacement of the first oscillator is increased, the spectrum of the second oscillator acquires the third subharmonic. Next comes a cascade of period-doubling bifurcations of this subharmonic until finally chaos sets in. We note that another avenue to the formation of chaos in the evolution of AE — through the onset of combination frequencies — could possibly be explained by increasing the number of oscillators in the proposed model.

- ¹V. A. Greshnikov and Yu. B. Drobot, *Acoustic Emission* [in Russian], Izd. Standartov, Moscow (1976).
- ²V. Z. Parton and V. G. Boriskovskii, *Dynamic Fracture Mechanics* [in Russian], Mashinostroenie, Moscow (1985).
- ³V. V. Krylov, *Akust. Zh.* **29**, 790 (1983) [*Sov. Phys. Acoust.* **29**, 468 (1983)].
- ⁴V. V. Krylov, E. P. Ponomarev, and S. I. Sidorova, "Influence of surface waves propagating along the edges of a crack on the acoustic emission spectra," in: *First All-Union Conference on Acoustic Emission of Materials*

and Structures, Proceedings [in Russian], Part 1, Rostov-on-Don (1984), pp. 30-31.

⁵V. V. Krylov and A. P. Ponomarev, *Akust. Zh.* **32**, 622 (1986) [*Sov. Phys. Acoust.* **32**, 386 (1986)].

⁶A. I. Markushevich, *Short Course in the Theory of Analytic Functions* [in Russian], Nauka, Moscow (1978).

Translated by J. S. Wood

Calculation of an acoustic field in a coastal zone of the ocean with an intricate bottom relief

A. N. Nekrasov

N. N. Andreev Acoustics Institute, Russian Academy of Sciences

(Submitted January 29, 1992)

Akust. Zh. **39**, 123-126 (January-February 1993)

A new tracing technique is described for rays joining a source and receiver in the propagation of sound in a coastal wedge with an intricate bottom relief, where the sound velocity depends only on the depth. It is established that a significant gain in computing speed can be achieved by concentrating the receivers in a limited region of space. Examples of calculations are discussed.

The calculation of acoustic fields in the ocean with an intricate bottom relief is still an underdeveloped activity, despite the fair number of papers (e.g., Refs. 1-3) on methods and algorithms designed to solve this complex problem. The main difficulty is the large volume of calculations needed to determine the acoustic field in situations of practical interest. For example, ray tracing requires the emanation of an enormous number of rays from the source within the limits of a prescribed sector of angles of emergence in order for neighboring rays to be of the same type and thus to ensure convergence of the iterative scheme⁴ used to find the ray incident on

the receiver. In some cases the "fan" of rays must have a density of 100 rays per degree both in the azimuth angle and in the vertical angle. This means that millions of rays are needed in order to calculate the acoustic field in the entire water region covered by the rays.

It is not always necessary, however, to calculate the acoustic field in the entire region under investigation. If a large number of receivers is used, it is theoretically possible to simplify the problem on the basis of *a priori* information about the angle of emergence of rays leaving the source and entering the vicinities of the receivers. In practice, however, such information is very difficult to obtain. Nonetheless, a major simplification of the problem can be achieved on this basis in at least one case, which is described below. Results of calculations will also be given.

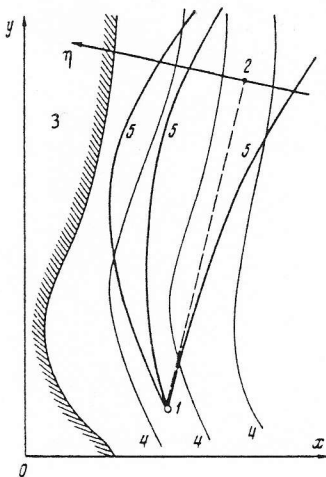


FIG. 1. Deviation of horizontal projections of ray paths from the position of the receiver array. 1) Source; 2) site of the vertical line array of receivers; 3) shore; 4) isobaths; 5) horizontal projections of ray paths. The η axis is orthogonal to the line 1-2.

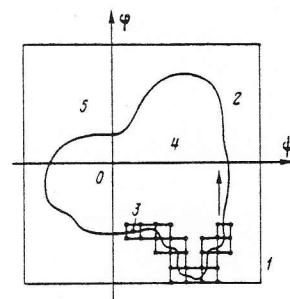


FIG. 2. Tracing around a limit ring. a) Sector of angles of emergence; 2) limit ring; 3) starting point for tracing; 4) region in which $\eta < 0$; 5) region in which $\eta > 0$. The dots represent the points at which the ray paths are calculated in the plane of angles of emergence.